View metadata, citation and similar papers at core.ac.uk

brought to you by CORE

provided by HAL-CEA

Synergetic effects of collisions, turbulence and sawtooth crashes on impurity transport

X Garbet, Jae-H Ahn, S Breton, P Donnel, D Esteve, R Guirlet, H Lütjens, T Nicolas, Y Sarazin, C Bourdelle, et al.

To cite this version:

X Garbet, Jae-H Ahn, S Breton, P Donnel, D Esteve, et al.. Synergetic effects of collisions, turbulence and sawtooth crashes on impurity transport. 2016. <hal-01367373>

HAL Id: hal-01367373

https://hal.archives-ouvertes.fr/hal-01367373

Submitted on 16 Sep 2016

HAL is a multi-disciplinary open access archive for the deposit and dissemination of scientific research documents, whether they are published or not. The documents may come from teaching and research institutions in France or abroad, or from public or private research centers.

L'archive ouverte pluridisciplinaire **HAL**, est destinée au dépôt et à la diffusion de documents scientifiques de niveau recherche, publiés ou non, émanant des établissements d'enseignement et de recherche français ou étrangers, des laboratoires publics ou privés.

Synergetic effects of collisions, turbulence and sawtooth crashes on impurity transport.

X. Garbet[1], J.H. Ahn[1], S. Breton[1], P. Donnel[1], D. Esteve[1], R. Guirlet[1], H. Lütjens[2], T. Nicolas[3], Y. Sarazin[1], C. Bourdelle[1], O. Février[1], G. Dif-Pradalier[1], P. Ghendrih[1], V. Grandgirard[1], G.Latu[1], J.F. Luciani[2], P. Maget[1], A. Marx[2], A. Smolyakov[4]

[1] CEA, IRFM, F-13108 Saint Paul-lez-Durance, France.
[2] Centre de Physique Théorique, Ecole Polytechnique, CNRS, France.
[3] National Institute for Fusion Science, Nagoya 464-01, Japan.
[4] University of Saskatchewan, Saskatoon, S7N 5E2 Canada.

e-mail contact of main author: xavier.garbet@cea.fr

Abstract This paper investigates the interplay of neoclassical, turbulent and MHD processes, which are simultaneously at play when contributing to impurity transport. It is shown that these contributions are not additive, as assumed sometimes. The interaction between turbulence and neoclassical effects leads to less effective thermal screening, i.e. lowers the outward flux due to temperature gradient. This behavior is attributed to poloidal asymmetries of the flow driven by turbulence. Moreover sawtooth crashes play an important role to determine fluxes across the $q = 1$ surface. It is found that the density profile of a heavy impurity differs significantly in sawtoothing plasmas from the one predicted by neoclassical theory when neglecting MHD events. Sawtooth crashes impede impurity accumulation, but also weaken the impurity outflux due to the temperature gradient when the latter is dominant.

1 Introduction

Impurity transport is a subject of renewed interest due to several facts. First plasma facing components made of tungsten are currently tested in several tokamaks, in view of a future implementation in Iter. This has triggered an active research on means to prevent influxes of heavy impurities. Furthermore, burning plasmas will produce helium, which should be expelled from the plasma core and pumped. Finally impurities with medium charge number are commonly injected in the scrape-off layer to cool down the edge plasma. These impurities should be prevented from reaching the plasma core to avoid dilution and excessive radiative losses. These constraints raise questions on the mechanisms that underlie impurity transport for various mass and charge numbers. It turns out that collisional, turbulent and MHD processes are simultaneously at play and contribute to impurity transport. It is shown here that these contributions are not additive, as assumed sometimes. Moreover the interplay between turbulence, neoclassical and sawtooth crash effects leads to less effective thermal screening, i.e. a weakening of the outward flux due to temperature gradient.

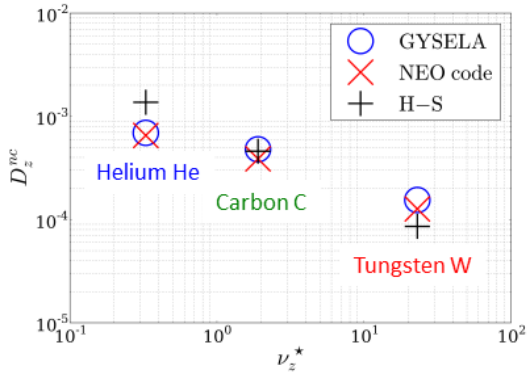

Figure 1: *Neoclassical diffusion coefficients vs ν_Z^* calculated with the GYSELA code, NEO code and analytical theory*

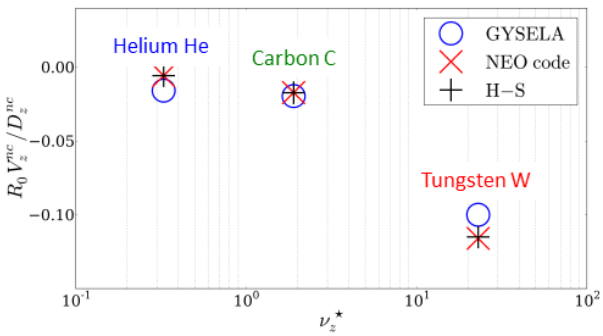

Figure 2: *Neoclassical pinch velocities vs ν_Z^* calculated with the GYSELA code, NEO code and analytical theory*

2 Neoclassical and turbulent impurity transport

It is reminded that the neoclassical impurity flux is given by the following expression

$$\Gamma_{Z\psi} = -D_Z^{nc}\frac{\partial N_Z}{\partial r} + V_Z^{nc} N_Z$$

where N_Z is the impurity density. The ratio of the pinch velocity V_Z^{nc} to the diffusion coefficient D_Z^{nc} is of the form $\frac{V_Z^{nc}}{D_Z^{nc}} = Z\frac{\partial \ln N_i}{\partial r} + HZ\frac{\partial \ln T_i}{\partial r}$, where N_i and T_i are the ion density and temperature. The number H is the thermal screening factor and is equal to $-\frac{1}{2}$ when the impurity is in the Pfirsch-Schlüter regime, while the main ion species is in the banana-plateau regime. A multi-species collision operator has been implemented in the GYSELA gyrokinetic code, in order to compute neoclassical and turbulent particle fluxes on an equal footing [1]. It has been benchmarked against the theory of neoclassical transport [2] and the NEO code [3, 4]. The agreement is found to be satisfactory for both the diffusion coefficient and the pinch velocity for various collisionality regimes (see Fig.1 and Fig.2).

The upgraded version of the GYSELA code has been run above the instability threshold of Ion Temperature Gradient driven modes (ITG) [5]. It is found that neoclassical and turbulent processes contribute to impurity transport in a complex manner. This question has been assessed as follows. Three simulations are run for each impurity :

1. Purely neoclassic (called "neoclassic" hereafter): in this case, all non-axisymmetric toroidal modes are filtered out at each time step (i.e. all Fourier modes with $n \neq 0$ are set to zero, with n the toroidal mode number). The neoclassical flux is then the sum of both $\mathbf{v}_E$ and magnetic drift $\mathbf{v}_D$ contributions:

$$\langle \Gamma_z^{neo} \rangle_\psi = \left\langle \int d^3\mathbf{v}\ F_z\ (\mathbf{v}_{D,z} + \mathbf{v}_{E,z}^{n=0}) \cdot \boldsymbol{\nabla} r) \right\rangle_\psi \tag{1}$$

2. Mainly turbulent (called "turbulent" hereafter): in this case, single-species collisions only are retained (namely ν_{ii} and ν_{zz}) , so that momentum or energy exchange be-

tween species are not taken into account. Retaining intra-species collisions is important and sufficient to account, among others, for the collisional damping of zonal flows, which are known to contribute efficiently to turbulence self-regulation. In the case of trace impurities, the collision operator for the main ions only is important. Indeed, impurity-impurity collisions are negligible in this case. The turbulent flux is then governed by the electric drift:

$$\left\langle \Gamma_z^{turb} \right\rangle_\psi = \left\langle \int d^3\mathbf{v}\ F_z \left(\mathbf{v}_{E,z} \cdot \boldsymbol{\nabla} r \right) \right\rangle_\psi \tag{2}$$

3. Full (called "total" hereafter): in this case, no simplification is made to the collision operator, nor any filtering applied to the electric potential. More precisely, all terms of the collision operator are retained, involving both intra- and inter-species collisions, in the turbulent regime.

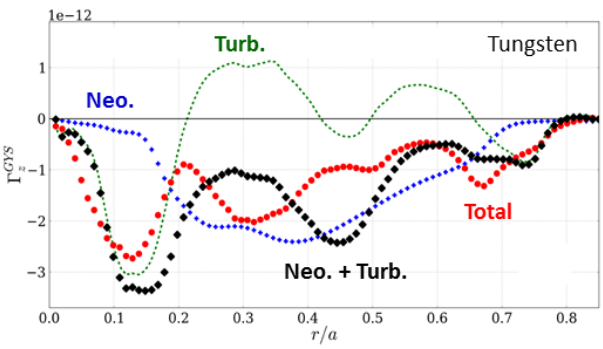

Figure 3: *Neoclassical (blue) and turbulent (green) fluxes calculated separately, and their sum (black) compared to the self-consistent total flux (red)*

As an example, the case of tungsten is considered hereafter. The same trend is observed for other impurities. In Fig.3 the total tungsten flux (red) from the self-consistent simulation is compared to the sum (black) of the neoclassical (blue) and turbulent (green) fluxes, that come from the reduced simulations. It appears that the total flux differs from the sum of the neoclassical and turbulent fluxes, by more than a factor two at some radial locations. This result shows that neoclassical and turbulent impurity transports are not additive. One explanation for this synergy comes from the impact of turbulence on the magnitude and radial shape of in/out poloidal asymmetries. The pattern of the impurity density in the poloidal plane is a signature of this multiscale dynamics. The left panel of Fig.(4) shows the level of $n = 0$ fluctuations of impurity density, while the right panel shows non axisymmetric $n \neq 0$ small scale fluctuations. A similar structure is observed for the electric potential. Small scale fluctuations are clearly modulated by $n = 0$ perturbations. Conversely, it is expected that turbulence generates $n = 0, m = \pm 1$ perturbations (m is the poloidal wave number), that produces a significant contribution to neoclassical transport. The interplay

via large scale flows is expected to be a key mechanism to explain the synergistic effects that are observed.

Moreover the coefficient of thermal screening, which quantifies the outward pinch due to the temperature gradient, is above the neoclassical value $H = -\frac{1}{2}$ in presence of turbulence, and can become positive. This is an unfavorable configuration, as it may lead to impurity accumulation. This behavior is attributed to the same mechanism, i.e. poloidal asymmetries of the flows driven by turbulence, via a mechanism similar to the effect of poloidal asymmetries (e.g. centrifugal force or potential asymmetries produced by RH heating). Such asymmetries are able to greatly modify neoclassical coefficients, up to one order of magnitude, as predicted theoretically [6, 7].

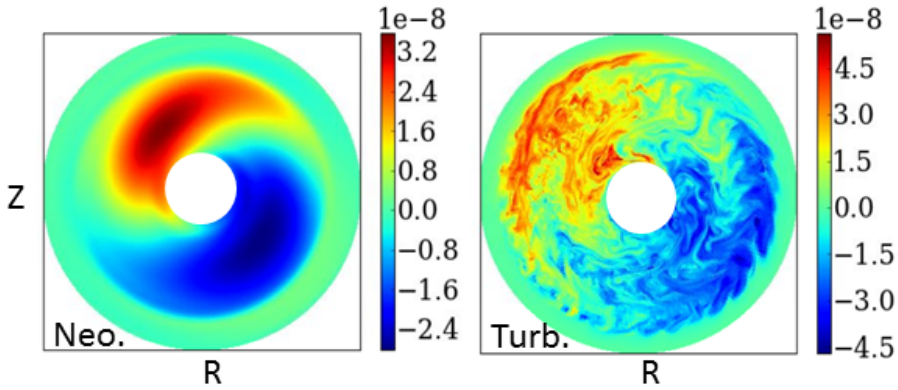

Figure 4: *Poloidal map of tungsten density fluctuations in a GYSELA gyrokinetic simulation. left panel:* $n = 0$ *axisymmetric fluctuations. right panel:* $n \neq 0$ *non-axisymmetric fluctuations*

3 Effect of sawtooth crashes on impurity transport

The interplay of neoclassical transport and sawtooth events has been assessed by implementing a set of fluid equations in the XTOR-2F code [8], which model the impurity flows and are consistent with the gyrokinetic model in the collisional regime. The impurity density and parallel momentum equation read

$$\partial_t N_z + \nabla \cdot (N_z \mathbf{V}_z) + \left(\nabla \times \frac{\mathbf{B}}{B^2} \right) . \frac{\nabla P_z}{e_z} = S_z \tag{3}$$

$$N_z m_z \left(\partial_t V_{\|,z} + (\mathbf{V}_z \cdot \nabla) V_{\|,z} \right) = -\nabla_\| P_z + N_z e_z E_\| + R_{\|,zi} \tag{4}$$

where N_z and $\mathbf{V}_z$ are the impurity density and fluid velocity, e_z and m_z the charge and mass, S_z is the impurity density source, and $R_{\|,zi}$ is the parallel friction force given by

$$R_{\|,zi} = -m_z N_z \nu_{zi} (V_{\|,z} - V_{\|,i}) - \frac{2}{5} C_0 m_z N_z \nu_{zi} \frac{Q_{\|,i}}{P_i} \tag{5}$$

where $V_{\|,i}$ and $Q_{\|,i}$ are the main ion parallel velocity and heat flux. Turbulent diffusion and pinch velocities can be added via an ad-hoc diffusion/convection transport model in Eq.(3). Banana-plateau neoclassical transport coefficients can be added in the same manner. However the Pfirsch-Schlüter neoclassical flux should not be added in that way since it is already accounted for in the fluid equations Eqs.(3,4) . The expression of the collisional drag force Eq.(5) is essential in that regard. Using the Braginskii value of $C_0 = 1$ would be a mistake, since no thermal screening is found when all species (main ion and impurity) are in the Pfirsch-Schlüter regime [10]. The appropriate choice of C_0 to recover the correct value $H = -\frac{1}{2}$ is $C_0 = \frac{3}{2}$, which is the one that has been implemented in the XTOR code. It has been verified that the profiles of impurity density agree with the neoclassical predictions in MHD quiet plasmas.

Once the Eqs.(3,4) have been implemented and verified, the XTOR-2F code has been

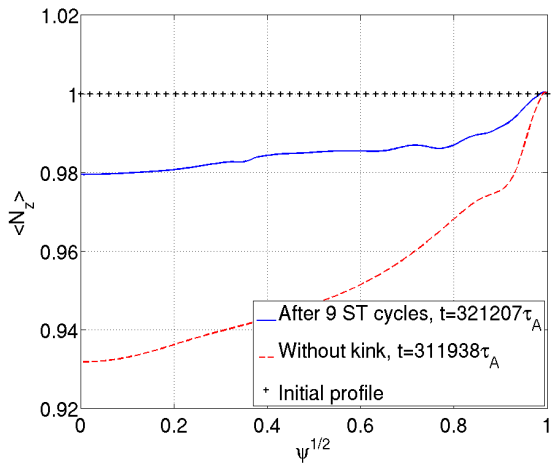

Figure 5: *Impurity profile with (blue line) or without sawtoothing activity (red line). The impurity neoclassical flux is outward due to thermal screening.*

run in a regime of parameters where a steady sawtoothing regime sets on [11]. It is found that the impurity density behaves differently with or without sawteeth [9]. Typically the impurity density profile is less peaked than the one computed without sawtooth collapses. This is due to the flattening effect of sawtooth crashes. Neoclassical relaxation processes are negligible during a crash, since they are too slow. Conversely neoclassical transport is the prominent transport channel during the recovery phase. Hence the interplay comes from modifications of the profiles during the crash, which persist during the recovery phase, thus modifying neoclassical fluxes. When the main ion density gradient is large $|\nabla N_i/N_i| \geq |\nabla T_i/2T_i|$, the neoclassical pinch velocity is directed inward, but sawtooth crashes fight against it and impede impurity accumulation, a well known result. However when the temperature gradient is dominant $|\nabla N_i/N_i| \leq |\nabla T_i/2T_i|$ so that the neoclassical pinch velocity points outward, sawteeth fight against profile depletion and therefore *weaken the thermal screening effect*. An example is shown in Fig. 5, where parameters have been

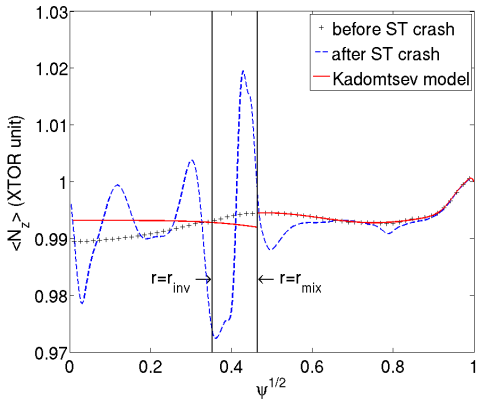

Figure 6: *Comparison of the final impurity profile to Kadomtsev model for an initial slightly hollow profile*

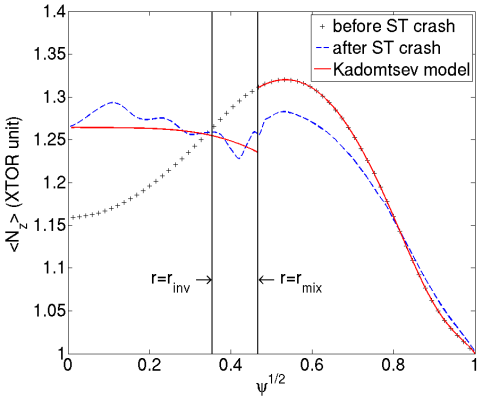

Figure 7: *Comparison of the final impurity profile to Kadomtsev model for an initial hollow profile*

chosen such that the impurity neoclassical flux is outward due to thermal screening. It appears clearly that the impurity profile after 9 crashes is less hollow than the one obtained without sawteeth, i.e. with neoclassical transport alone.

For practical purposes, it is interesting to compare the post-crash profiles with those predicted by the Kadomtsev reconnection model [14, 15, 16]. The final impurity profile differs from the one predicted by the Kadomtsev reconnection model when the pre-crash impurity density profile is slightly depleted. This is due to sawteeth induced corrugations of the density, which are clearly seen in XTOR-2F simulations after each crash (see Fig.6). Density perturbations also appear on the main ion post-crash density, and have been observed by fast-sweeping reflectometry tomography on Tore Supra [12]. On the contrary, the post-crash impurity profile is consistent with the Kadomtsev prediction when the pre-crash profile is hollow (Fig.7), as already found in [13]. The agreement is not perfect though.

During the crash, the impurity transport dynamics is quite complex. In particular, it appears that impurities are concentrated after the crash within an annulus in between the inversion and mixing radii, while fine structures develop inside the inversion radius [13, 9]. The flux can be decomposed in two components: one due to the perpendicular fluid $E \times B$ drift velocity (the diamagnetic component is negligible for high Z impurities), and the other one due to magnetic flutter. These fluxes are defined as follows

$$\mathbf{\Gamma}_{z,\delta B} = N_z V_{\parallel,z} \frac{\delta \mathbf{B}}{B} \tag{6}$$

and

$$\mathbf{\Gamma}_{z,E} = N_z \mathbf{V}_E \tag{7}$$

It is found that the radial flux due to $E \times B$ drift is much larger than the contribution of magnetic flutter in most places (see Fig.8 and Fig.9). Hence fine structures are due to convection, not to magnetic flutter.

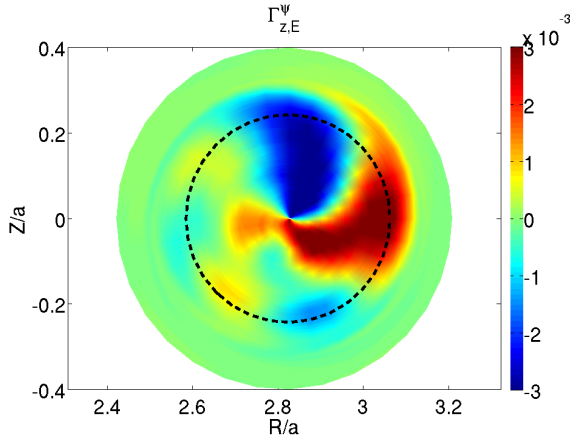

Figure 8: *Radial flux due to $E \times B$ drift velocity during a sawtooth crash*

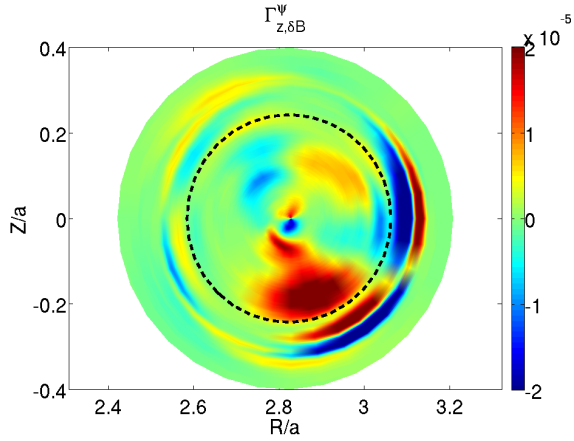

Figure 9: *Radial flux due to magnetic flutter during a sawtooth crash*

4 Conclusion

In summary, it appears that collisions, turbulence and MHD processes contribute synergistically to impurity transport, thus questioning the usual assumption of additivity. The interplay between turbulent and neoclassical transport has been studied with the GYSELA gyrokinetic code, which has been equipped with a comprehensive collisional operator. It is found that the impurity flux found in a self-consistent simulation differs from the sum of neoclassical and turbulent fluxes calculated separately. This behavior is attributed to poloidal convective cells generated by turbulence, which modify neoclassical fluxes. Hence synergy is the result of poloidal asymmetries and interaction between disparate scales. Moreover the thermal screening effect gets weaker. The two fluid non linear MHD code XTOR-2F has been modified to model the dynamics of heavy impurities. The collisional drag force has been adjusted such that the Pfirsch-Schlüter impurity flux agrees with the one predicted by neoclassical theory, including the thermal screening term. Simulations of sawtoothing plasmas indicate that the time average impurity profile is flatter than the one predicted by neoclassical theory alone. This is equivalent to a weakening of the thermal screening term in situations where the outward pinch velocity due to temperature gradient dominates over the contribution of the density gradient responsible for accumulation. The post-crash profiles are reasonably in agreement with those predicted by the Kadomtsev reconnection model, when pre-crash profiles are sufficiently contrasted. Fine structures of the impurity density develop during the crash and persists some time. These structures results from small scale convective scales associated with the crash dynamics. The overall impurity profile relaxation is controlled by the $E \times B$ convection.

Acknowledgments

This work has been carried out within the framework of the EUROfusion Consortium and the French Research Federation for Fusion Studies and has received funding from the Euratom research and training programme 2014-2018 under grant agreement No 633053. We benefited from HPC resources from GENCI, and IFERC.

References

[1] D. Estève, X. Garbet, Y. Sarazin, et al., Physics of Plasmas **22**, 122506 (2015).

[2] S.P. Hirshman and D.J. Sigmar, Nucl. Fusion **21**, 1079 (1981).

[3] E. Belli and J. Candy, Plasma Phys. Control. Fusion **50**, 095010 (2008)

[4] E. Belli and J. Candy, Plasma Phys. Control. Fusion **54**, 015015 (2012).

[5] D. Estève, X. Garbet, Y. Sarazin, et al., submitted to Nucl. Fusion (2016).

[6] F. Fülöp and P. Helander, Physics of Plasmas **6**, 3066 (1999).

[7] C. Angioni and P. Helander Plasma Phys. Control. Fusion **56**, 124001 (2014).

[8] H. Lütjens and J.-F Luciani *J. Comp. Phys.* **229**, 8130 (2010).

[9] J.H. Ahn et al., submitted to Plasma Phys. Control. Fusion.

[10] P. H. Rutherford *Phys. Fluids* **7**, 1782 (1974).

[11] F.D. Halpern, H. Lütjens and J.-F Luciani *Phys. Plasmas* **18**, 102501 (2011).

[12] T. Nicolas, R. Sabot, X. Garbet, H. Lütjens, and J.-F. Luciani, Physics of Plasmas **19**, 112305 (2012).

[13] T. Nicolas, H. Lütjens, J.-F. Luciani, X. Garbet, and R. Sabot, Physics of Plasmas **21**, 012507 (2014).

[14] B.B. Kadomtsev Sov. J. Plasma Phys. **1**, 389 (1975) [Fiz. Plasmy **1**, 710 (1975)] .

[15] F. Porcelli, D. Boucher and M.N. Rosenbluth Plasma Phys. Control. Fusion **38**, 2163 (1996).

[16] I. Furno *et al* Nucl. Fusion **41**, 403 (2001).